energies

MDPI

Review

The Hydration and Volume Expansion Mechanisms of Modified Expansive Cements for Sustainable In-Situ Rock Fragmentation: A Review

Janethri Buddhipraba Liyanage and Ranjith Pathegama Gamage *

Department of Civil Engineering, Deep Earth Energy Laboratory, Monash University, Building 60, Melbourne, VIC 3800, Australia; janethri.paranaliyanage@monash.edu
* Correspondence: ranjith.pg@monash.edu; Tel.: +61-399054982

Abstract: This review provides the hydration and volume expansion mechanism of expansive materials, with the goal of utilizing them in the development of sustainable mining methods. The main focus of the review will be the newly developed non-destructible rock fragmentation method, slow releasing energy material agent (SREMA), which is a modified soundless chemical demolition agent (SCDA). The review aims to address one of the main gaps in studies related to SREMA, by presenting a thorough understanding of the components of SREMA and their mechanisms of action, leading to volume expansion. Thus, this review would act as a guide for researchers working on using expansive materials for rock breaking. As many literatures have not been published regarding the recently discovered SREMA, studies on cements, expansive cements, and soundless chemical demolition agents (SCDA) were mainly considered. The chemical reactions and volume expansive processes of these materials have been studied and incorporated with the additives included in SREMA, to understand its behavior. Literature containing experimental studies analyzing the heat of hydration and microstructural changes have been mostly considered along with some of the heavily discussed hypotheses regarding the hydration of certain components, to predict the volume expansive mechanism of SREMA. Studies related to SREMA and other similar materials have shown drastic changes in the heats of hydration as the composition varies. Thus, SREMA has the capability of giving a wider range of expansive energies in diverse environmental conditions

Keywords: slow releasing energy material agent (SREMA); preconditions; rock fragmentation; soundless chemical demolition agent (SCDA); volume expansion; hydration mechanism; viscosity enhancing agent (VEA); high range water reducer (HRWR)

Citation: Liyanage, J.B.; Gamage, R.P. The Hydration and Volume Expansion Mechanisms of Modified Expansive Cements for Sustainable In-Situ Rock Fragmentation: A Review. *Energies* **2021**, *14*, 5965. https://doi.org/10.3390/en14185965

Academic Editor: José A.F.O. Correia

Received: 14 July 2021
Accepted: 15 September 2021
Published: 20 September 2021

1. Introduction

As of 1970, the global population has doubled and the human lifestyle has become much more sophisticated, leading to the exploitation of energy sources and natural resources. Mining is one of the oldest man-made methods developed to acquire the lushness of earth, and continues to play a massive role providing energy, chemical, pharmaceutical, and construction resources and much more. Rock fragmentation, the initial step of mining, can be performed in several different ways such as explosive blasting, hydraulic fracturing, and electrical disintegration. However, these techniques can cause severe environmental impacts [1–4]. For example, the Global Resources Outlook of 2019 reported that about 37% of the impact in climate change and 7% of loss in biodiversity have been caused by metal, non-metal and fossil fuel extraction alone. Thus, forging the path for innovative extraction techniques while meeting the concepts of sustainable development is highly in need.

In search of an eco-friendlier solution of mining, basic expansive cement which was generally used to compensate the volume shrinkage in concrete and include tensile stress in reinforcement [5], has evoked much interest in the research community. The components of expansive cements are similar to Portland cement, containing mostly CaO,

and Al_2O_3, SiO_2, MgO, Fe_2O_3, $CaSO_4$ in smaller amounts. Expansive cement would emit heat when interacting with water, resulting in an expansion in volume as an impact of the hydration products. Extensive studies have been conducted to understand the volume expansion mechanism [6–8] and the effect of ambient temperature, bore diameter, and amount of water [9] on expansive cements, which have led to the development of soundless chemical demolition agents (SCDA) for the cracking and destruction of cement-based structures [10–12]. Here, the expansive force caused by the hydration of the SCDA would cause fracturing in the confined material, as it exceeds the force exerted by it.

However, when considering deep-earth mining and hydrocarbon extraction, which goes about five kilometers into the earth, this formula cannot be directly used. This is mainly as expansive cements would tend to dilute in the presence of high-water content, eventually leading to the wash off of the product and uncontrolled hydration [13]. Over the past few decades, elementary SCDAs have been developed into modified SCDA [13], also known as slow releasing energy material agent (SREMA), with the incorporation of additives such as superplasticizers, viscosity enhancing agents and accelerators. This formula has been patented by Gamage et al. as an improved demolition agent [14]. Unlike conventional fracturing techniques, SREMA does not cause any noise or explosions, generate fly rocks, vibrate, or produce toxic gases. Additionally, SREMA shows multiple radial fractures around the injection point, unlike the uneven fracturing of rock-blasting and single-fracture splitting of hydraulic fracturing.

When SREMA is injected into the targeted zone via a borehole, it undergoes expansion causing fractures in the surrounding materials and exposing the fossil fuel, metals, minerals, or ores of interest, that may lie within. This pre-treatment opens the rock, creating microfractures, which leads to the efficient extrusion of natural resources as the exposed area would be large. In-situ leaching can be done for metal recovery, where a lixiviant can be circulated through the created channels, allowing the dissolution of the metal and transportation of the liquid back to the surface for further treatment [15,16]. Similarly, SREMA can also be adopted for hydrocarbon recovery [17] and geothermal energy extraction [18–20].

In this review, we shall discuss the components of SREMA and their role in the volume expansion towards sustainable rock fragmentation and mining. Due to the recent discovery of SREMA, not many studies have been conducted on it or its behavior. Thus, cements, expansive cements and SCDAs have been taken into consideration to predict its mechanisms of action and the performance of additives. A molecular scale understanding of SREMA would aid in the further development of the composition, to obtain the necessary expansive pressure for specific ground conditions and cover the gap in studies.

2. Volume Expansion and Rock Fracturing through Expansive Materials

The expected volume expansion by an expansive cement, leading to rock fragmentation, is mainly due to the hydration of CaO [21,22]. The formation of $Ca(OH)_2$ results in an increase in temperature to approximately 150 °C, due to the exothermic nature of the hydration reaction [9]. Yet, the volume expansion is not only caused by the exothermic heat expelled, but would also depend on the crystallization of $Ca(OH)_2$ and ettringite ($Ca_6Al_2(SO_4)_3(OH)_{12}{\cdot}26H_2O$).

The volume expansion from the reactants to the products can simply be understood by the molar mass and specific gravity of the reactants and products. As clearly seen in Table 1, the molar volume increases as CaO hydrates to $Ca(OH)_2$ and then to ettringite. It is therefore obvious that the expansion of volume is directly correlated to the degree of hydration of CaO. This suggests that the amount of CaO in the system would have a direct impact on the amount of energy produced by an expansive material.

Table 1. Molar volume calculation.

Chemical Component	Molar Mass/ $\times 10^{-3}$ kg mol^{-1}	Specific Gravity/ $\times 10^{3}$ kg m^{-3}	Molar Volume/ $\times 10^{-6}$ m^{3} mol^{-1}
CaO	56.1	3.34	16.8
$Ca(OH)_2$	74.1	2.24	33.1
Ettringite	786.7	1.77	444.5

However, the volume expansion can be understood more broadly by the theories on nucleation and crystal growth [7,23]. The swelling theory explains both the formation and lengthening of $Ca(OH)_2$ crystals around the hydrating CaO causing the volume expansion, assuming that the expansion occurs with the adsorption of water. The crystal growth theory considers the volume expansion with the formation of crystals. When SREMA is wetted, the solution would be saturated with Ca^{2+} and OH^- ions, which would initiate the growth of small $Ca(OH)_2$ crystals, of approximately (10–20) nm, around the hydrating CaO surfaces [24]. As the solubility of CaO increases, the crystal size would grow further and after a certain point, the growth would be detained, as the crystals grow in a confined environment, thereby causing an outward thrusting pressure. This pressure depends on the molar volume of the forming crystals, saturation of the solution and the absolute temperature. According to the Shalom's model, the expansive volume is much more affected when the solid crystals themselves come in contact and restrain the growth of each other [6,7].

The volume expansion also depends on the ettringite formation, which occurs in the presence of $CaSO_4$. According to Dessouki et al. [25], the incorporation of 15% $CaSO_4$ to SCDA of Betonamit brand delayed the point of maximum volume expansion (5.5 h) compared to that of plain SCDA (3.5 h), but a much greater significant volumetric expansion was observed in the presence of $CaSO_4$.

With the aim of increasing the expansive force generated and thereby the crack propagation, studies have been conducted using large percentages of CaO compared to the 82% seen in commercial SCDA. Kasei et al. with over 90% CaO [26], and Ishii et al. with 88% CaO [27], have shown that this would also increase the heat of hydration creating a steam blowout, which would be unpredictable and thus quite dangerous. Therefore, to boost the rate of volumetric expansion without violent reactions, adjustments have been made to the SCDA systems by mixing in other cementing compounds such as tricalcium silicate, also known as alite ($3CaO{\cdot}SiO_2$), and tricalcium aluminate ($3CaO{\cdot}Al_2O_3$). Another reason for the addition of these minerals, which are well known for their expansive properties when interacted with water, is the highly unstable nature of CaO under ambient conditions.

As the internal expansive force exceeds the force exerted by the confining material, the rock fracturing would be initiated. The rock failure mode may vary depending on the nature of the applied force, the resistance towards rock fragmentation and the fracture toughness. The most commonly considered mode would be the tensile crack opening (mode I), shearing (mode II) and tearing (mode III) [28]. As for SREMA, the rock fracturing would be mainly caused by mode I failure due to the hoop stresses that form around the injection well, thus resulting in a complex network of microfractures around the borehole. However, depending on the types of rocks or minerals on the mining ground, the failure point would differ, leading to the necessity of varying expansive forces. The large fracture network would depend on how the energy is transferred from one rock or mineral body to another with consideration to the boundaries that may be in between.

In summary, the expansive nature of expansive materials is proportional to the amount of CaO in the system. The crystallization of products occurring under confined conditions would cause the outward thrusting pressure. This pressure would lead to rock failure. However, the use of pure CaO is not favorable, thus requiring a well-constructed composition for expansive materials.

3. Components of SREMA

Considering the composition of SREMA, it has four basic components, which are the elementary SCDA mixture, welan gum as the viscosity enhancing agent, sodium naphthalene sulfonate formaldehyde (SNSF) as the high range water reducer (HRWR) and calcium chloride as the accelerator [13]. Yet, SREMA can be further developed depending on the SCDA used, to cater the ground and environmental conditions that need to be met.

As shown in Table 2, commercially available SCDA is mainly composed of CaO and smaller amounts of Al_2O_3, SiO_2, Fe_2O_3, MgO and $CaSO_4$. However, these mass percentages tend to differ from one SCDA brand to another.

Table 2. Chemical composition of SCDA.

Chemical Component	Percentage by Mass (%)
CaO	81–96
Al_2O_3	0.3–5.0
SiO_2	1.5–8.5
Fe_2O_3	0.2–3.0
MgO	0–1.6
$CaSO_4$	0.6–4.0

The aluminate and silicates are incorporated in the form of the earlier mentioned expansive minerals. Calcium sulfate, introduced as gypsum, is used to delay the hardening of concrete in the cement industry. However, considering the expansive properties, $CaSO_4$ is much more important in the formation of ettringite. The addition of pure SiO_2 would decrease the specific heat capacity and increase the thermal conductivity [29] and Fe_2O_3 would increase the strength of the mortar [30], leading to a more efficient expansive energy generation. However, unmodified SCDA tends to dilute in water-saturated conditions, leading to mass loss and delay in the volume expansion process [31]. This drawback has been overcome by using welan gum as the viscosity enhancing agent, to produce a hydrophobic barrier.

Welan gum is an anionic exopolysaccharide from the Sphingan family, containing a repeat unit of L-rhamnose, D-glucose and D-glucuronic acid, with either L-rhamnose or L-mannose attached to the third carbon of (1→4) bonded glucose unit, in an approximately 2:1 ratio [32]. It is a non-gelling polysaccharide [33]. This is quite useful in the cement industry as it can increase the retention of water and reduce the mass loss in the cement composition [34] and increase the viscosity when mixed with a HRWR [35]. Thus, SNSF is used on behalf of improving the workability, without excessively increasing the viscosity [36]. The interaction between welan gum and the HRWR would also result in appropriate properties for SREMA to be used underwater and in oil wells [37].

However, the reduction of mass loss by welan gum has a negative effect on the hydration of tricalcium aluminate in the presence of gypsum [38], inhibiting volume expansion. Therefore, an accelerator must be used to overcome the deceleration observed.

To accelerate the system, calcium chloride, a commonly used accelerator in the cement industry, has been found to be satisfactory [39,40]. However, increasing the amount of $CaCl_2$ does not increase the expansive energy, but rather shows an immediate volume expansion as soon as the slurry is mixed, giving a low expansive energy peak and remaining at a constant but poorer level [13].

The detailed mechanisms of the action of these components are discussed in the later sections.

4. Hydration Mechanism of Expansive Components of SREMA

As highlighted in the earlier section, the main volume expansive step of SREMA is the formation of $Ca(OH)_2$ and ettringite. These products are a result of the hydration of the SREMA constituents. Thus, the hydration process has much importance in this scenario. First, we will review the work performed on the hydration of each component separately to identify how it assists the overall volume expansion.

4.1. Hydration of Calcium Oxide

The hydration reaction of CaO is relatively straightforward giving $Ca(OH)_2$ one of the main volumetric phases [41].

$$CaO_{(s)} + H_2O_{(l)} \rightarrow Ca(OH)_{2\,(s)} + 15.2\ kJ/mol \quad (1)$$

This reaction is exothermic, releasing energy to the system, which would assist in the thermal expansion and the acceleration of the hydration due to the increase in temperature in the confined space.

However, pure CaO, produced by the thermal decomposition of limestone, bio skeletons or shells containing $CaCO_3$, at a temperature of about 800 °C, would easily convert back by the favorable reverse reaction, under ambient conditions with the considerable amounts of carbon dioxide.

$$CaCO_{3\,(s)} + heat \rightleftharpoons CaO_{(s)} + CO_{2\,(g)} \quad (2)$$

Thus, SREMA must not be in direct contact with the atmosphere for prolonged periods of time, if not used.

4.2. Hydration of Alite

Considering the hydration of alite, it would provide a substantially high amount of heat than that of CaO and would facilitate the production of $Ca(OH)_2$ through the formation of an intermediate product known as the calcium silicate hydrate (CSH). Initially, CSH would have a poor crystalline structure with sheets of calcium and oxygen with chains of tetrahedral silica, separated by water layers, forming atomic structure similar to tobermorite or jennite but with a higher Ca:Si ratio [42]. Yet, with further hydration, CSH would grow in the form of micro-needles around the tricalcium silicate surface until complete coverage is reached [43].

4.2.1. Molecular Scale Hydration Mechanism of Alite

To study the formation of the volume expansive phase via the hydration products, molecular-scale hydration was considered based on the conducted by Pustovgar et al., who suggested a proton transfer that occurs in the interface of the solid surface and water [44]. Here the tricalcium silicate surface has been broken down as follows, disregarding any impurities and surface deformations. This mechanism has been divided into 4 main steps,

1. Dissolution of tricalcium silicate.

$$3CaO{\cdot}SiO_{2\,(s)} + 3H_2O_{(l)} \rightleftharpoons 3Ca^{2+}{}_{(aq)} + 4OH^-{}_{(aq)} + H_2SiO_4{}^{2-}{}_{(aq)} \quad (3)$$

2. Proton abstraction by the surface oxide groups from the surrounding water molecules.

$$3Ca^{2+}{}_{(surface)} + SiO_4{}^{4-}{}_{(surface)} + O^{2-}{}_{(surface)} + H_2O_{(l)} \rightleftharpoons 3Ca^{2+}{}_{(surface)} + SiO_4{}^{4-}{}_{(surface)} + OH^-{}_{(surface)} + OH^-{}_{(aq)} \quad (4)$$

3. Formation of hydrated silicates with further proton transfer.

$$3Ca^{2+}{}_{(surface)} + SiO_4{}^{4-}{}_{(surface)} + OH^-{}_{(surface)} + OH^-{}_{(aq)} + H_2O_{(l)} \rightleftharpoons 3Ca^{2+}{}_{(surface)} + HSiO_4{}^{3-}{}_{(surface)} + OH^-{}_{(surface)} + 2OH^-{}_{(aq)} \quad (5)$$

$$3Ca^{2+}{}_{(surface)} + HSiO_4{}^{3-}{}_{(surface)} + OH^-{}_{(surface)} + 2OH^-{}_{(aq)} + H_2O_{(l)} \rightleftharpoons 3Ca^{2+}{}_{(surface)} + H_2SiO_4{}^{2-}{}_{(surface)} + OH^-{}_{(surface)} + 3OH^-{}_{(aq)} \quad (6)$$

$$3Ca^{2+}{}_{(surface)} + H_2SiO_4{}^{2-}{}_{(surface)} + OH^-{}_{(surface)} + 3OH^-{}_{(aq)} + H_2O_{(l)} \rightleftharpoons 3Ca^{2+}{}_{(surface)} + H_3SiO_4{}^-{}_{(surface)} + OH^-{}_{(surface)} + 4OH^-{}_{(aq)} \quad (7)$$

4. Formation of $Ca(OH)_2$.

$$3Ca^{2+}{}_{(surface)} + H_3SiO_4{}^-{}_{(surface)} + OH^-{}_{(surface)} + 4OH^-{}_{(aq)} \rightleftharpoons Ca(OH)_{2\,(s,\,interface)} \downarrow + 2Ca^{2+}{}_{(surface)} + H_3SiO_4{}^-{}_{(surface)} + 3OH^-{}_{(aq)} \quad (8)$$

As the reaction proceeds, more hydroxyl groups would become available in the solution, due to the proton abstraction from water, thus resulting in a change in basicity. Therefore, the reaction progress can be measured in terms of the pH of the surrounding aqueous layer.

The above mechanism has been further extended by the author to explain the formation of CSH.

5. Formation of CSH.

$$2Ca^{2+}{}_{(surface)} + H_3SiO_4{}^-{}_{(surface)} + 3OH^-{}_{(aq))} + H_2O_{(l)} \rightleftharpoons (CaO)_2SiO_2{\cdot}4H_2O_{\,(s,\,interface)} \downarrow \quad (9)$$

To clarify the validity of the mechanism, the overall reaction is considered, from steps (1)–(4), as follows,

$$3CaO{\cdot}SiO_{2\,(s)} + 5\,H_2O_{(l)} \rightarrow Ca(OH)_{2\,(s)} + (CaO)_2SiO_2(H_2O)_{4\,(s)} \quad (10)$$

Considering the overall reaction put forward by Taylor [45] for the formation of calcium hydroxide and CSH from tricalcium silicate, stoichiometric ratios of the formed CSH were calculated, which were quite encouraging, agreeing to the nearest integer, thus confirming the above mechanism.

$$3CaO{\cdot}SiO_{2\,(s)} + 5.2\,H_2O_{(l)} \rightarrow 1.2\,Ca(OH)_{2\,(s)} + (CaO)_{1.8}SiO_2(H_2O)_{4\,(s)} \quad (11)$$

Looking deeper in to steps (2) and (3), it can be seen that a Ca^{2+} ion has been seized out from the surface for the formation of $Ca(OH)_2$, creating voids on the tricalcium silicate surface. These voids, or etch pits, are energetically active and would act as a host for particles with a similar size to Ca^{2+} ions, to be adsorbed. These activated nucleation sites have led to one of the most promising hypotheses regarding the hydration of alite, and this will be discussed later in this section.

4.2.2. Time-Dependent Hydration Mechanisms of Alite

Although the previously discussed molecular scale mechanism supports the overall reaction suggested by Taylor, it has been proposed considering a completely pure form with uniform surfaces dissolving stoichiometrically. However, when considering the lattice structures, as shown in Figure 1, it can be clearly seen that the surfaces do not always obey the stoichiometric ratios. Furthermore, the electrical nature of the ions, even of similar chemical nature, may be different, resulting in uneven adsorption, nucleation and finally product formation. Therefore, the variations observed from Taylor's equation of the tricalcium silicate hydration discussed in the previous section, can be attributed to these assumptions.

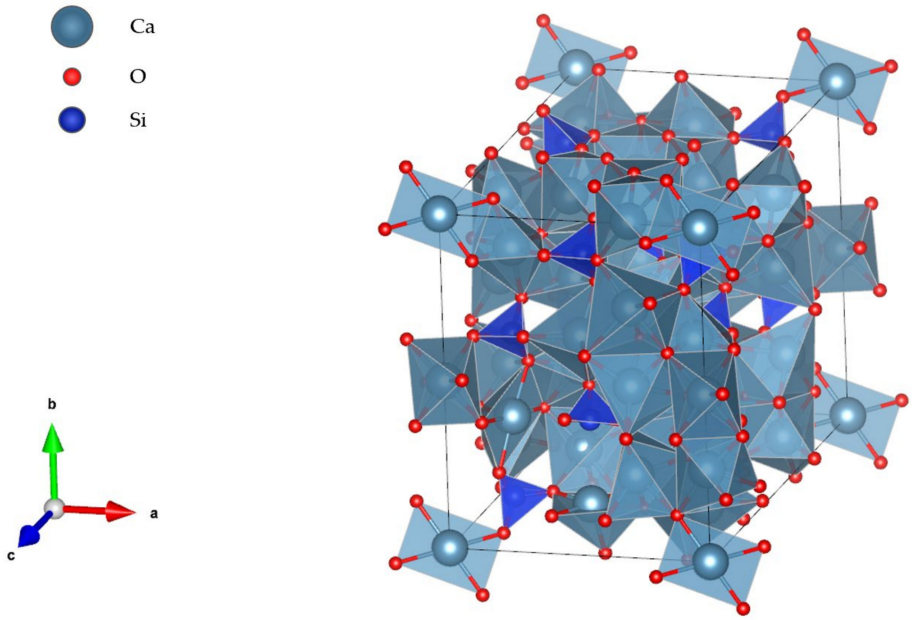

Figure 1. The lattice structure of tricalcium silicate (modified from [46]).

Considering the thermodynamics of the reaction between alite and water, a high heat of hydration is observed within the first few seconds. The reaction would then reduce during about 30 min and remain at a constant low rate of less than 1 mW/g. This steady state would last for about 1–2 h and would be consequently led to slow expansion. By the end of this period, the rate of hydrolysis would again increase at about 2 h into the hydration, reaching a secondary maximum at around 9 h, before gradually decreasing again [47]. Thus, five distinct stages can be seen in the hydration of alite, as shown in Figure 2.

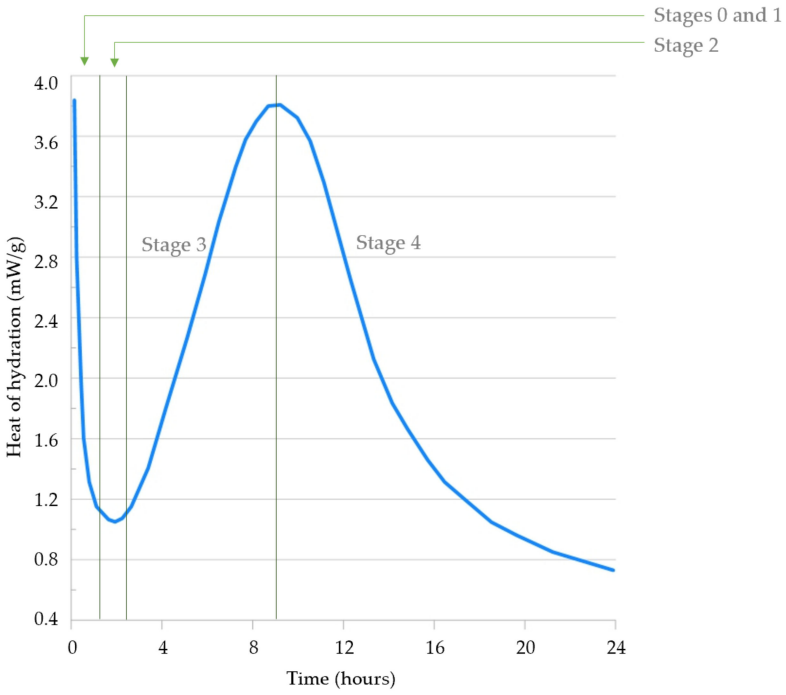

Figure 2. Experimental rate of hydration of alite(modified from [47]).

The rapid dissolution of the alite in water is a highly exothermic reaction, releasing a heat of about 138 kJ/mol immediately after wetting [47]. This would result in the initially observed high rate of Stage 0.

As the Ca^{2+} concentration increases with time, further dissolution would be inhibited by the Le' Chaterlier's principle, leading to the next stage of the hydration. However, by the end of Stage 0, the expected Si and Ca concentrations would be much lower when compared to the theoretical $K_{sp} \approx 3$ and the deceleration of the rate would occur in undersaturated conditions [48]. In addition, the molar ratio of Ca:Si observed during the steady state is much larger than the expected 3:1 ratio [49]. Thus, the rapid decrease in rate (Stage 1) in undersaturated conditions and the steady state (stage 2), which can be assumed to be an equilibrated period showing larger Ca:Si ratios, is an enigma. There are several hypotheses on this regard, but we shall review two of the most plausible mechanisms.

Protective Barrier Hypothesis

The protective barrier hypothesis states that there is a rapid formation of a thin metastable layer of the less soluble CSH, of a lower stoichiometric ratio when compared with alite [50], which acts as a barrier for water to diffuse and hydrate the alite, and to control the diffusion of particles from the unhydrated surfaces as well [51]. However, a considerable rate of hydration can be seen during this period (Stage 1), indicating that the reaction continues beneath the formed protective barrier suggested by this hypothesis, until an equilibrium is reached. To explain this, Gartner et al. [52] suggested the formation of two layers, one by the hydration of alite and the other by the precipitation from the surrounding solution. It has also been suggested that these layers would eventually turn into a stable form. The end of the steady state where an acceleration in rate is observed is predicted to occur as the stable barrier breaks due to the arising osmotic pressure. The origin of this pressure is explained by the difference between the ion concentration of the solution, which is in contact with the cement grains, and that of outside the barrier [53]. However, this theory has not gained much evidence to be proven correct.

Furthermore, the thermodynamically stable passivating layer formed on the unhydrated cement has never been observed by any experimental analysis, including atomic force microscopy conducted on flat calcium silicate surfaces under water and ionic solutions [54,55] and high-resolution electron microscopy on dried samples [56]. The difference in crystallographic orientation and the lack of an epitaxial relationship between the layer is considered as the barrier. Thus, the unhydrated alite surface, similar to a corroding metal surface and its protective oxide layer, suggests grey areas of this hypothesis.

Therefore, it can be said that the protective barrier hypothesis would only be able to explain the first two stages of the experimental observations, and a graphical representation of this hypothesis can be plotted as indicated in Figure 3.

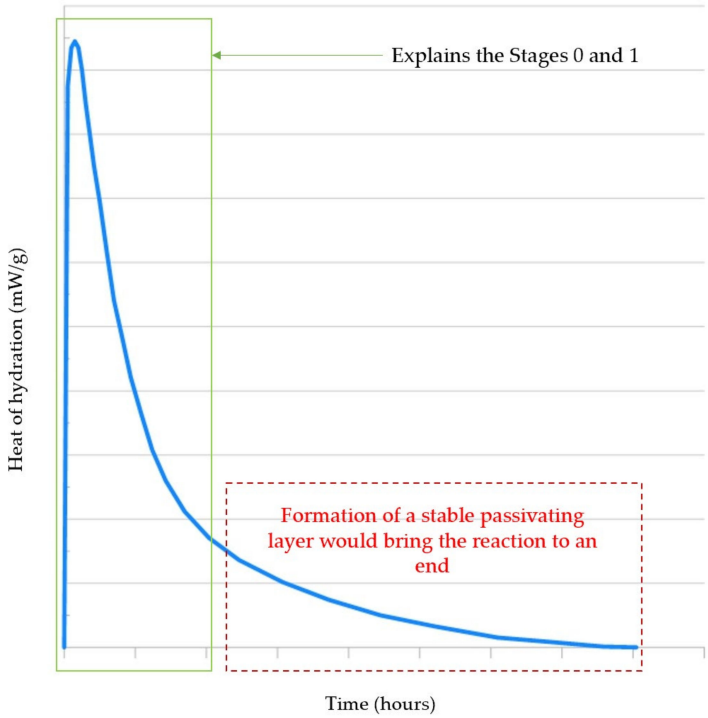

Figure 3. Expected rate of hydration by the protective barrier hypothesis.

Slow Dissolution Hypothesis

Another hypothesis that has been developed is the controlled dissolution hypothesis. Here the dissolution mechanism would depend on the degree of saturation. At very high levels of undersaturation of $Ca^{2+}_{(aq)}$, prior to equilibration, which is at about (10–20) mmol/L [49], the dissolution rate would be very high, which enables an etch pit activation on the surface, and thus defects the surface. As the undersaturation decreases and reaches equilibrium, the etch pit openings occur in a negligibly small scale. After this point, the rate of dissolution would depend on the previously activated etch pit density, thus ensuring slow release of the ions from the activated etch pits. This will lead to a decelerating dissolution rate and then a steady state [57]. An additional reason for the decreasing rate, which leads to a constant low stage, is the poisoning of the etch pits by the free silicate ions in the solution [58].

However, this deceleration can be expected to be more of a dragged tail. This is due to the availability of active CSH nucleation sites, unlike in the case of the protective barrier hypothesis where the active surface is said to be entirely covered by an impermeable membrane.

It is possible to consider the impure nature of alite to explain the experimentally observed sharp deceleration. Alite, being the impure form of tricalcium silicate, contains small amounts of Al_2O_3, MgO, Fe_2O_3, P_2O_5, Na_2O, and K_2O. As Al_2O_3 is insoluble in water it would therefore not have any effect on the hydration reaction. However, MgO can easily react with water, to form a gel-like barrier of $Mg(OH)_2$ around the unreacted alite [59].

$$MgO_{(s)} + H_2O_{(l)} \rightarrow Mg(OH)_{2\,(s)} \quad (12)$$

The formation of this barrier would cause a delay in the expansion [60] to result in the sudden drop in the heat evolution in Stage 1, as observed experimentally. The slight solubility of Mg(OH) can be used to believe that the barrier layer is faintly permeable to water and this penetrable nature would allow the CSH formation to take place with the activation of etch pits, but at a slow steady level (Stage 2). Eventually, the needle-shaped CSH would tear the $Mg(OH)_2$ barrier, exposing the unreacted alite, resulting in an acceleration in hydration.

Moreover, the growth of the intermediate product CSH would cause a reduction in the Si concentration, thus increasing the molar ratio of Ca:Si. This explains the experimentally observed characteristic of the steady state mentioned earlier. The decrease in Si concentration would also open up the etch pits that were previously poisoned and facilitate the precipitation of $Ca(OH)_2$, thus increasing the degree of unsaturation of Ca^{2+} with respect to CSH. This would again activate the dissolution of tricalcium silicate and offer a greater driving force for the CSH formation [61], explaining the accelerating Stage 3. In addition, as discussed in the earlier section, ettringite would contribute to the volume expansion of SREMA and provide greater nucleation sites for the CSH growth, thus ensuring a more rapid hydration.

The steady state of Stage 2 is hypothesized to be the time between the slow dissolution process and the increasing growth rate of CSH. Considering the silicate concentration drop in the beginning of the hydration, this proves that the CSH begins to form during the first few minutes of hydration, controlling the hydration kinetics [62,63]. During Stage 2, CSH would start to form and once they reach a certain critical size, would provide a more active surface area for further heterogeneous nucleation, and the start of the acceleration period could be observed. Therefore, it can be concluded that the Stages 2 and 3 are controlled by the nucleation and growth of hydrates, which are coupled with the dissolution of tricalcium silicate, where the main peak of heat release is caused by the precipitation of CSH and $Ca(OH)_2$.

In order to explain the deceleration seen in Stage 4, Bazzoni [43] proposed that when forming new needles, CSH would not form on top of the originally formed needles but would form in the interfaces between the needles and the anhydrous grains. Therefore, a lowering in the diffusion of ions through the hydrate leading to a lowered growth rate was hypothesized. This hypothesis seems to coincide with the Dijon model, as it states that CSH grows both parallel and perpendicular to the surface until full coverage is reached and then only grows perpendicularly afterward [64].

4.3. Hydration of Tricalcium Aluminate

The other most important component of SREMA is tricalcium aluminate ($3CaO{\cdot}Al_2O_3$). Its hydration would mainly govern the setting time and the workability of a basic Portland cement mixture. Similarly, with more hydration, the fluidity and the strength of the expansive cement may be lost. Therefore, gypsum ($CaSO_4{\cdot}2H_2O$), as a form to introduce sulfates, is added to control this reaction.

4.3.1. In the Absence of Sulfates

In the absence of sulfates, the hydration of tricalcium aluminate can be divided into two stages: (1) dissolution of tricalcium aluminate and (2) formation of metastable hydration products within the first few minutes of the reaction. These hydration products first form a gel-like structure on top of the tricalcium aluminate surface. This would develop into an intermediate hydrate of plate-like structure and eventually form hexagonal structured $Ca_3Al_2O_6.6H_2O$ between 8–24 h into the hydration [65].

$$2\ Ca_3Al_2O_{6\,(s)} + 27\ H_2O_{(l)} \rightarrow Ca_4Al_2O_7{\cdot}19H_2O_{(s)} + Ca_2Al_2O_5{\cdot}8H_2O_{(s)} \quad (13)$$

$$2\ Ca_3Al_2O_{6\,(s)} + 21\ H_2O_{(l)} \rightarrow Ca_4Al_2O_7{\cdot}13H_2O_{(s)} + Ca_2Al_2O_5{\cdot}8H_2O_{(s)} \quad (14)$$

$$Ca_4Al_2O_7{\cdot}19H_2O_{(s)} + Ca_2Al_2O_5{\cdot}8H_2O_{(s)} \rightarrow 2\ Ca_3Al_2O_6{\cdot}6H_2O_{(s)} + 15\ H_2O_{(l)} \quad (15)$$

The SEM images of the hydration products, indicating the morphological changes are shown in Figure 4 below.

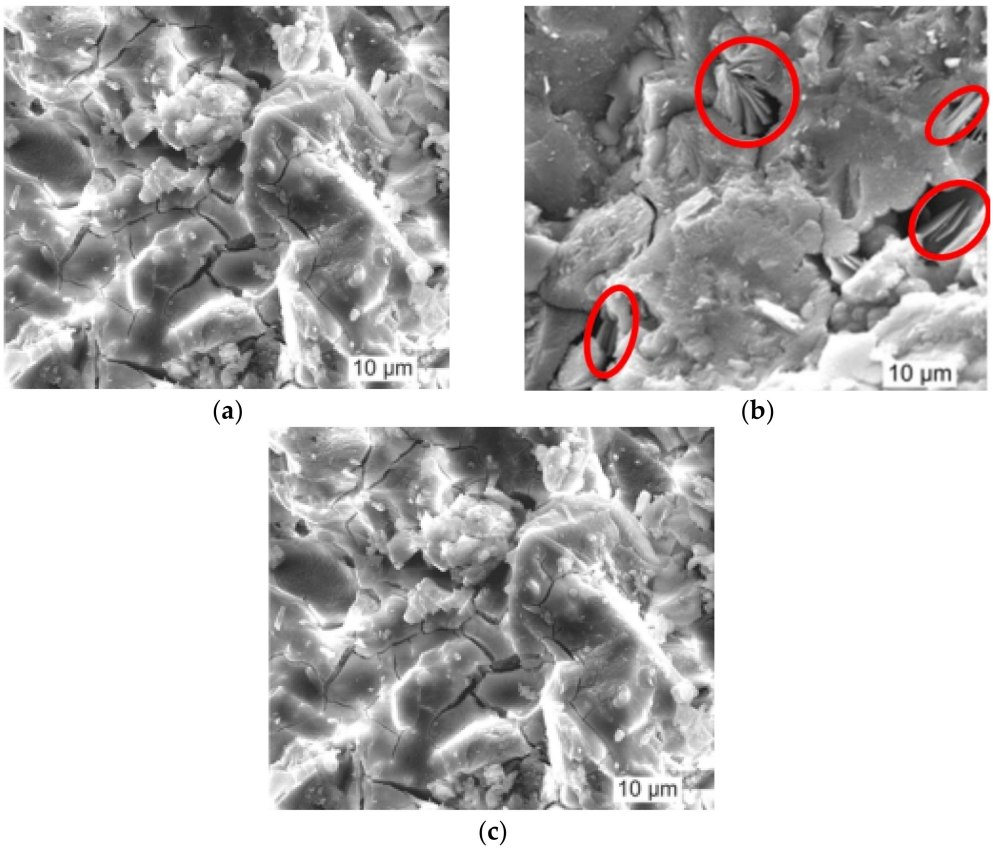

(**a**) (**b**)

(**c**)

Figure 4. SEM images of the hydration products in the absence of sulfates giving: (**a**) gel-like hydration products covering the tricalcium aluminate surface (~5 min), (**b**) plate-like intermediated hydrates (~1 h), and (**c**) hexagonal platelet-like hydration products (8–24 h) [66].

During the hydration of tricalcium aluminate, the formed gel layer would act as a barrier disrupting the hydration of the main volume expansive components. Since it is a fast reaction compared to others of the cement mixture, it also uses up all the water to give more calcium aluminate hydration products, leading to the flash set. The formation of the gel layer will be completed in minutes; hence the flowability of the SREMA is highly affected by the hydration of tricalcium aluminate. In addition, having aluminum ions in the solution can increase the steady state and disrupt the hydration of alite. This is either due to the adsorption of aluminum ions onto alite, diminishing its solubility [67], or the formation of Calcium Aluminum Silicate hydrates (CASH) that would not enable the seeding of CSH for further growth [68].

The retardation of alite solubility in the presence of aluminates have been further studied by Pustovgar et al. [44] using various dosages of $NaAlO_2$. They have concluded that aluminates tend to adsorb on to the active sites of alite promoting the formation of hydrated calcium aluminate (AFm phase) in the form of $[Ca_2(Al,Fe)(OH)_6]\cdot X\cdot xH_2O$, where X is an exchangeable singly or doubly charged anion [69], enhancing the aluminum incorporation in CSH and increasing the amount of CASH. These observations agree with the slow dissolution hypothesis as it acknowledges the effect of etch pit activation on the changes observed in the reaction rate.

4.3.2. In the Presence of Sulfates

Even with the adverse effects of tricalcium aluminate, it is quite useful, when used in the presence of sulfates, for the volume expansion expected in SCDA as it forms ettringite crystals within the gel structure. In the presence of sulfates, the hydrolysis process can be divided into two main peaks and a deceleration period as presented in Figure 5.

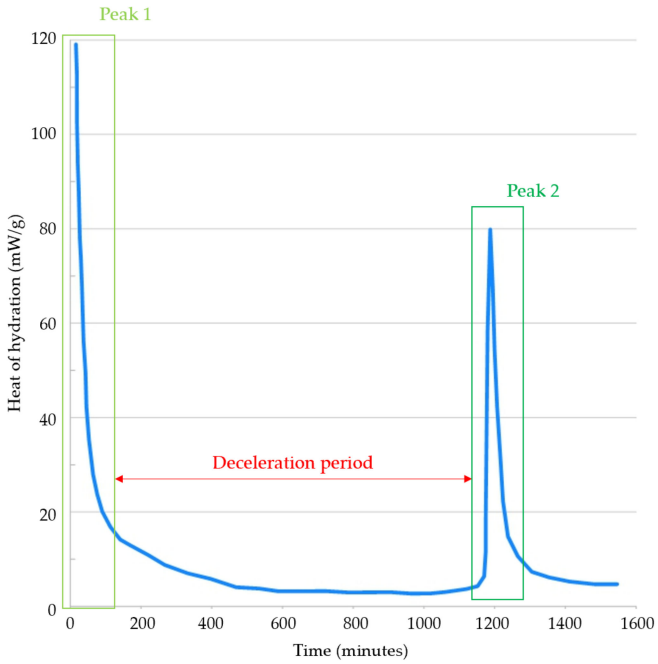

Figure 5. Rate of hydration of tricalcium aluminate with 45% sulfates by mass of tricalcium aluminate (modified from [47]).

Similar to the hydration of alite, the initial high release of heat can be observed expelling approximately 160 mW/g of heat, irrespective of the amount of sulfates added [70]. Next, the dissolution and rapid precipitation of ettringite complete within a few minutes, leading to the deceleration. The formation of ettringite, occurring at a sulfate concentration of 12.5 mmol/L with respect to portlandite, takes about five minutes to be first observed.

$$Ca_3Al_2O_{6\,(s)} + 3CaSO_4{\cdot}2H_2O_{(s)} + 26\,H_2O_{(l)} \rightarrow Ca_6Al_2(SO_4)_3(OH)_{12}{\cdot}26H_2O_{(s)} \quad (16)$$

It is believed that the deceleration occurs due to the impermeable nature of ettringite crystals which form on the tricalcium aluminate surface, retarding further hydration, until the sulfate concentration depletes [71].

In the presence of $CaSO_4$, depending on the degree of supersaturation and amount used, ettringite would show different morphologies from short hexagonal prisms to long needles [72]. These ettringite crystals can tear up the formed gel which would cause flash set. This would allow further hydration of the SCDA while maintaining the fluidity until the mixture has been transferred to the desired location.

In terms of how ettringite assists the volume expansion, Meredith et al. [65] have found that the length of the crystals formed depend on the water to solid ratio and longer crystals can be expected with the increase in the ratio. Accordingly, under 10% water to solid ratio with 25% gypsum by weight of tricalcium aluminate, large crystals of ettringite have been observed in the intergranular spaces within the first hour of the reaction. This observation can therefore be correlated with the increase in the volume expansion observed by increasing the water to solid ratio [9]. However, the larger size of the crystals can also be attributed to the saturation level that is ideal for the crystal growth and the space availability.

After the initial high heat of hydration, rapid deceleration can only be observed in the presence of sulfates. Two hypotheses have been proposed to explain the deceleration: (1) protective membrane hypothesis and (2) sulfate adsorption hypothesis.

The protective membrane hypothesis considers the formation of an ettringite or AFm phase protective barrier [73]. However, considering the needle-like structure of ettringite crystals, they might not have the capability to produce a complete coverage and the AFm precipitate can be seen even in the absence of externally added sulfates [74] unlike the

deceleration of Stage 2. The more possible explanation would be the adsorption of sulfates into the active sites of the tricalcium aluminate, with the dissolution of more gypsum to compensate the reduction in the sulfate concentration with the formation of ettringite. The adsorption of sulfates is assumed to be quite preferential, forming electrostatic interactions with the Ca^{2+} ions, showing higher nucleophilicity. Due to the distance between the two most nucleophilic Ca^{2+} ions being about 3.5 Å, which allows only one sulfate ion to house, the sulfate ions may be trapped in the active sites, which would explain the retarded hydration [75] by inhibiting the dissolution of tricalcium aluminate and nucleation around the active sites.

However, even after the deceleration, some amount of ettringite is formed in a slow rate (Stage 3), and it can be confirmed by the slow decrease in conductivity of the sample, from 11 mS/cm to slightly less than 10 mS/cm [70,76]. By the end of the Stage 3, the sulfate concentration would completely diminish and the ettringite would dominate the hydrated phase.

At this point, another sharp exothermic peak releases heat of about 90 mW/g. Here, the formed ettringite would react with the tricalcium aluminate producing calcium aluminum monosulfate hydrate [57].

$$2\ Ca_3Al_2O_{6\,(s)} + Ca_6Al_2(SO_4)_3(OH)_{12}\cdot 26H_2O_{(s)} \rightarrow 3\ Ca_4Al_2SO_{10}\cdot 12H_2O_{(s)} + 20\ H_2O_{(l)} \quad (17)$$

Compared to alite, which undergoes hydration for over 24 h, the hydration of tricalcium aluminate ends faster (about 9 h). However, it is clear that increasing the sulfate concentration would result in a longer time for it to diminish. Therefore, it becomes obvious that the length of Stage 2 and the characteristics of the calcium aluminum monosulfate hydrate formed during Stage 3 would greatly depend on the amount of sulfate added to the system. Studies have shown that while 6% gypsum containing samples showed the second hydration peak at about 100 min into the reaction, the samples with 43% gypsum took much longer and did not show the second peak until 1200 min into the hydration [70,76].

It has also been noted that the original form of the sulfates incorporated into the system influences the intermediate products of the reaction. If a hemihydrate such as $CaSO_4\cdot\frac{1}{2}H_2O$ is used, instead of gypsum, the initial hydration peak would show a lower heat maximum of about 95 mW/g, but a higher rate of ettringite formation, in the first 5 h of the reaction. This is due to the high solubility of hemihydrates leading to higher sulfate and calcium concentrations with respect to ettringite, favoring early ettringite nucleation and formation. In addition, if a hemihydrate were used, the formation of the hydroxy-AFm phase ($Ca_4Al_2(OH)_{12}\cdot 7H_2O$) would not be observed [70]. This is attributed to the high sulfate concentration which discourages the aluminum ions adsorption onto alite, instead of the rapid formation of ettringite.

4.4. Combined Hydration of Alite and Tricalcium Aluminate

The combined hydration of alite and tricalcium aluminate is dependent on numerous factors. These may be related to the chemical composition, for example, the amount of sulfate in the system or the ratio of alite to tricalcium aluminate, and the environmental conditions under which the reaction is studied. The following section provides a comprehensive discussion of the overall hydration mechanism.

4.4.1. Effect of Sulfate Concentration

In a system with sufficient amounts of sulfates, with over 2.4% by mass of SREMA [77], the reaction was observed to accelerate greatly during the nucleation and the crystal growth processes. This would lead the main alite peak about 7–8 h into the hydration. Soon after, a sharp peak, corresponding to the formation of monosulfate from tricalcium aluminate at the point of sulfate depletion, will be seen. Figure 6 depicts the overall rate of hydration of a properly sulfated system.

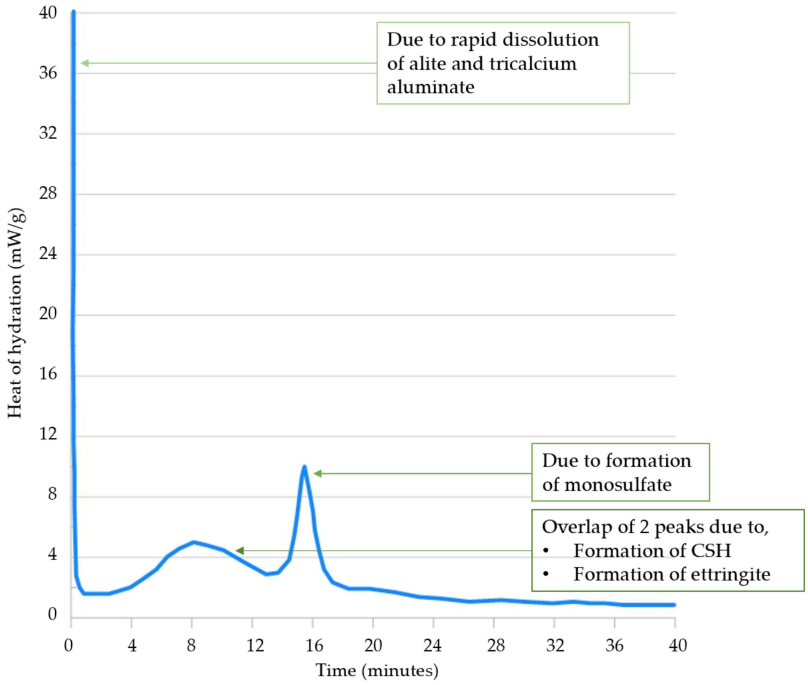

Figure 6. Overall rate of hydration of a properly sulfated system (modified from [57]).

Under low sulfate percentages with less than 1.3% by mass [47], the hydration of alite would be delayed while the monosulfate peak is seen much earlier. Thus, a clear relationship between alite hydration and sulfates can be observed and it is said to be due to the modifications to the growth of CSH by the adsorption of sulfate ions. That being said, EDS analysis indicates no such unique modification. However, the hydration of alite would retard in the presence of aluminates by the formation of the byproduct CASH. In the absence of active etch pits, aluminates tend to attack polar groups such as water, to form more a stable state $Al(OH)_3$ with a gel-like consistency. This has a solubility product K_{sp} in the range of $\sim 10^{-34}$, explaining its stability.

$$AlO_2{}^-{}_{(aq)} + 2H_2O_{(l)} \rightleftharpoons Al(OH)_{3\,(s)} + OH^-{}_{(aq)} \quad (18)$$

However, the reaction can be considered as a minor reaction in the presence of activated voids, giving a stable form of aluminates. The formation of CASH can be hypothesized as follows:

$$3Ca^{2+}{}_{(surface)} + H_3SiO_4{}^-{}_{(surface)} + 3OH^-{}_{(aq)} + H_2O_{(l)} + 2AlO_2{}^-{}_{(surface)} \rightleftharpoons (CaO)_3(Al_2O_3)(SiO_2)\cdot 4H_2O_{\,(s,\,interface)} \downarrow \quad (19)$$

As the exact composition of CASH is yet to be found, the mechanism cannot be validated by comparing the formulated composition and the actual value. However, this mechanism does align with the theory of how CASH formation minimizes the dissolution of alite, as more Ca^{2+} ions on the surface would be used up for the formation of CASH rather than the formation of $Ca(OH)_2$ and CSH, interrupting the volumetric phase.

Nonetheless, experimental evidence suggests that the alite peak would tend to be seen much earlier with the increase in sulfate percentage, when compared with that in the absence of sulfates [78]. However, an optimum condition is reached at 5% sulfate where the peak is observed about 7 h into the hydration, producing a maximum of about 4.5 mW/g of heat. After this point, increasing the sulfate concentration simply delayed the generation of the peak. These observations were explained considering that it is not the alite-sulfate system that accelerates the hydration, but sulfates using up the aluminates in the solution producing ettringite, that slow down the alite hydration. The deceleration of the reaction

after a certain sulfate concentration may be due to the sulfates attacking the active sites of alite, disrupting its solubility and thus the reaction rate.

Considering the overall heat of Portland cement, as indicated by Figure 7, the alite peak and the monosulfate peak appear to merge. Thus, the monosulfate peak is often confused with a shoulder peak seen in the main peak. This shoulder peak can be seen in the verge of the sulfate depletion, at which the tricalcium aluminate hydration is accelerated greatly, giving ettringite. It is assumed that the sulfates previously absorbed on to the CSH have depleted at this point [79].

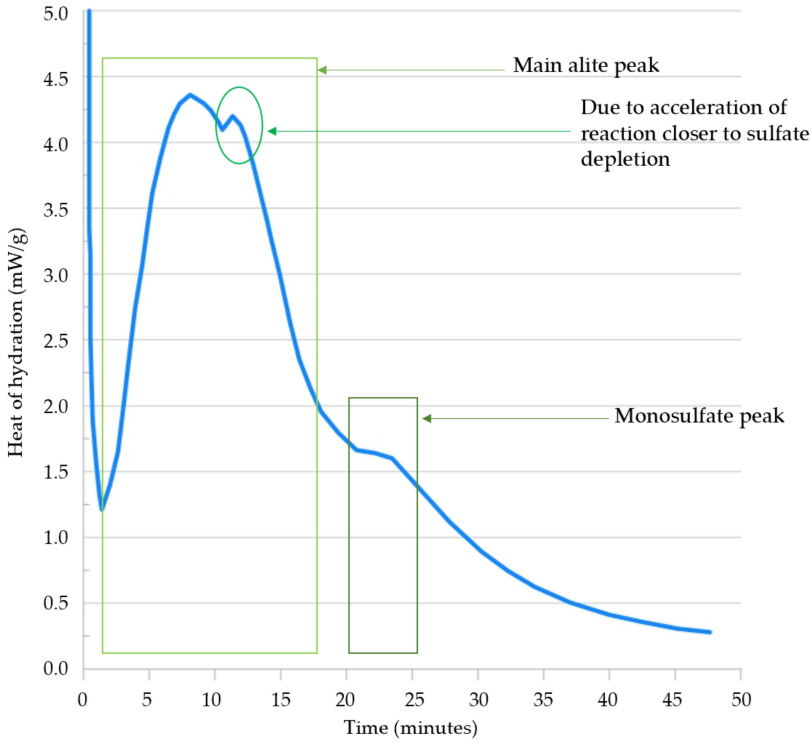

Figure 7. Rate of hydration observed for Portland cement (modified from [47]).

Thereafter, in the range of 20–30 h into the hydration, a low broad peak can be seen, and this is attributed to the formation of AFm phase. As discussed in the earlier section, the AFm phase has a chemical formula of $[Ca_2(Al,Fe)(OH)_6]\cdot X\cdot xH_2O$, where X is an exchangeable singly charged anion, such as chloride and hydroxyl ions, or doubly charged, such as carbonate and sulfate ions.

4.4.2. Effect of Alite to Tricalcium Aluminate Ratio

Studies have been carried out to understand the influence of the ratio of alite to tricalcium aluminate for the overall rate of hydration [78]. It has been found that the peaks corresponding to the alite hydration are barely influenced by small changes to the ratio. However, it has been observed that larger ratios would lead to an earlier monosulfate peak. While a 90:10 ratio of alite to tricalcium aluminate showed the monosulfate peak at around 43 h into the hydration, the sample with the ratio of 94:6 showed the same peak about 23 h earlier. As the ratio increases, the amount of corresponding tricalcium aluminate would be reduced and thereby the amount of sulfates incorporated into the system would also be reduced. The large amounts of alite would give an efficient CSH production, which then would adsorb a larger portion of the sulfates. This would ultimately lead to a sulfate deficiency and initiate the monosulfate formation [78].

4.4.3. Effect of Temperature

As for any chemical reaction, the reaction rate would increase with the temperature of the system. This can be attributed to the increased kinetic energy of the molecules, which then undergoes increased random chaotic motion with a larger number of successful collisions, forming the products with an increased rate. Additionally, as more molecules possess an energy equal to or greater than the activation energy of the reaction, much faster product formation can be seen.

The hydration kinetics of the combined mixture has been studied using isothermal calorimetry at 15 °C, 20 °C, 26 °C and 30 °C [78], and as expected the reaction occurs faster with increased temperature and the observed peak intensities are also higher. However, it has also been observed that a system containing adequate amounts of sulfate would act as an over-sulfated system at low temperatures and as an under-sulfated system at elevated temperatures [78]. This indicates that cements which are properly sulfated at room temperature may behave in an under-sulfated manner at higher temperatures.

To explain this observation, the activation energies for the hydration of alite and tricalcium aluminate with varying amounts of sulfates have been considered. Both activation energies tend to increase with the amount of sulfates added, and also may be related to the inhibition of the hydration mechanism by adsorbing into the CSH of alite and the active sites of tricalcium aluminate. However, at reduced levels of sulfate, the activation energy corresponding to the hydration of tricalcium aluminate is lower compared to alite. At elevated temperatures, the monosulfate formation would be much faster than alite hydration, acting as a highly under-sulfated system. Therefore, it can be concluded that under low sulfate concentrations, the hydration of tricalcium aluminate is more sensitive to the temperature.

It must also be noted that further improvements to the SREMA composition are necessary, especially to be used under high-temperature conditions in deep underground mining and geothermal energy excavations.

5. Additives of SREMA and Their Mechanisms of Action

Considering the composition of SREMA, while the compounds in abundance undergo a hydration reaction in the presence of water, the additives—welan gum, SNSF and calcium chloride—would not react with water but would instead follow independent mechanisms of action. Regardless, it is essential to study the behavior of these additives in water to avoid using up the water required for side reactions producing unnecessary byproducts, while intruding on the primary reactions of concern. Therefore, the nature of the chemical compound when exposed to free water molecules, chemical processes that make it a suitable additive, and its interaction with the other components of SREMA will be reviewed in this section.

5.1. Effect of Welan Gum

Considering SREMA shows its activity in the presence of water, welan gum should not disrupt the main reactions of concern, resulting in the volume expansion. Although welan gum has been studied extensively due to its commercial importance in many areas, the exact mechanism of it in water is poorly studied. Gellan gum, having the same tetrasaccharide backbone as welan gum [80], would act as a gelling agent forming a gel-like consistency with water and would disintegrate in the presence of excess of water. However, welan gum, having either L-rhamnose or L-mannose as a side group in glucose (*), is a non-gelling agent [33] which leads to a viscous aqueous solution rather than undergoing complete hydration. Therefore, it is safe to say that welan gum would not intervene with the hydration reactions of the main components, causing changes in the optimum amount of water incorporated.

As discussed earlier, welan gum has a repeat unit of D-glucose, D-glucuronic acid and L-rhamnose. Therefore, it is quite clear that a single repeat unit of welan gum has several equatorial -OH groups for the formation of hydrogen bonds. In the presence of

water, the molecules can be held strongly by these equatorial -OH groups, increasing the viscosity [32].

In the presence of water, welan gum would dissolve, showing polyelectronic properties due to the ionization of the D-glucoronic acid side chain [37].

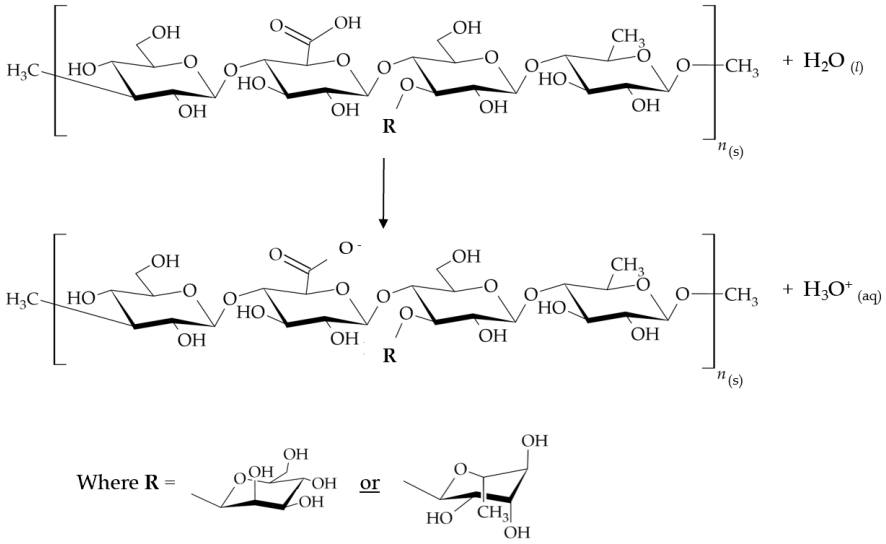

(20)

These ionizied carboxylate groups of the welan gum can bind strongly to the adsorption sites of the SREMA, from either tricalcium silicate [81] or tricalcium aluminate [38], causing a reduction in mass loss.

Ma et al. [38] considered two main stages of tricalcium aluminate to explain the retarding effect in the presence of welan gum: (1) the dissolution of tricalcium aluminate and (2) the consumption of sulfates leading to ettringite. It has been proposed that the anionic sites of welan gum would adsorb onto the surface of the tricalcium aluminate, disrupting the dissolution process and thereby affecting the $Ca(OH)_2$ saturation. Therefore, the nucleation and growth of ettringite would be hindered as the active sites would become unavailable for the incoming sulfate ions. Morphological analysis conducted by Ma et al. [38] suggests that the addition of welan gum would decrease the crystal size, giving a gel-like agglomerate with partial coverage of ettringite over tricalcium aluminate instead, while the gypsum particles tend to have a clean surface even 48 h into the reaction. Therefore, the sulfate consumption may stall leading to porous ettringite crystal, disrupting the volume expansion process with the incorporation of welan gum. Figure 8 indicates the differences in gypsum surfaces in the presence and absence of welan gum and how the morphology of ettringite is affected by it.

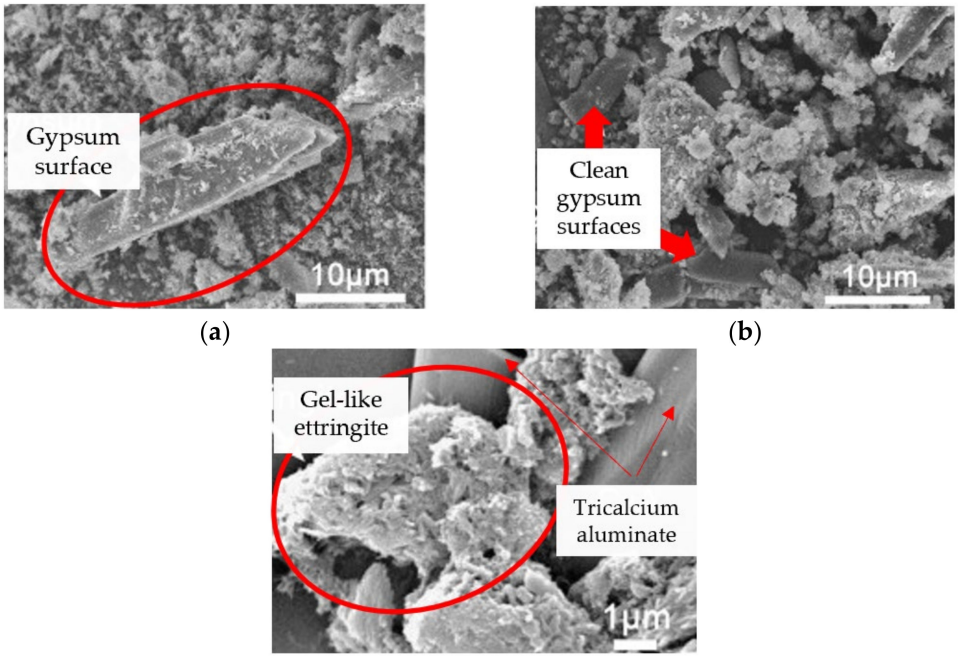

Figure 8. (**a**) SEM images of gypsum surfaces in the absence of welan gum. SEM images of (**b**) gypsum surfaces and (**c**) tricalcium aluminate surface partially covered with gel-like ettringite, in the presence pf 0.5% welan gum after 24 h into hydration [38].

5.2. Effect of SNSF

In the presence of water, SNSF would separate into sodium ions and naphthalene sulfonate formaldehyde condensate (NSF), which is an anionic surface-active agent [82]. Thus, there would be no hydration reactions that would interfere with the main volume expansive mechanism.

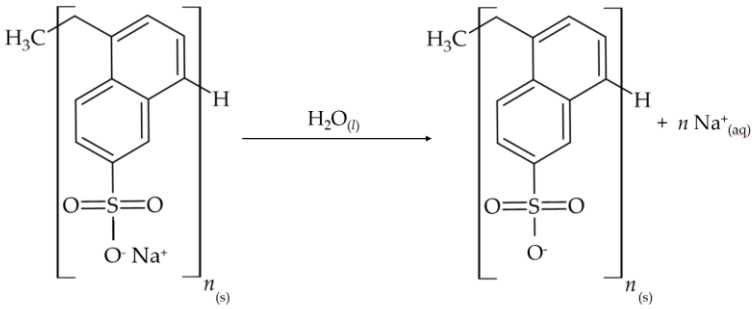

(21)

As any surfactant, the anionic molecules of SNSF would arrange the hydrophilic component interacts with water, causing a reduction in the surface energy by the separation of water molecules, thereby reducing the surface tension and improving the workability of the SREMA mixture.

According to Sakata et al. [35], when mixed well with a HRWR, welan gum would act as a liquified viscosity agent, which is caused by the swelling up of the welan gum particles, creating a stable suspension even without much of a viscosity increase. However, in the presence of cement particles, the naphthalene formaldehyde polycondensate would adsorb on to their surface [83,84], and with an increased adsorption, an increase in fluidity and reduction in fluid loss would be observed [85,86]. Thus, the amount of water necessary for the complete hydration of SREMA would be reduced. This adsorption due to the sulfonate group of the SNSF brings up the concern regarding its influence on the main hydration process, similar to welan gum. Many studies have shown that alite [87] and tricalcium

aluminate hydrations [88] are retarded in the presence of SNSF. Studies conducted by Hekal et al. [89] regarding the effect of SNSF on the formation of ettringite observed that it retards the reaction and leads to smaller crystal formation with increasing amounts of the sulfonated HRWR. However, an optimum level of 0.6% of SNSF has been seen by Collepardi et al. [90], where the hydration of tricalcium aluminate in the presence of gypsum has shown no difference to that in the absence of the admixtures.

Yet, the sulfonate group of the SNSF, being a comparatively weaker anchor than the carboxylate group of welan gum, can result in a decrease in the effectiveness as a superplasticizer [91].

5.3. Effect of Calcium Chloride

Calcium chloride is used in the SREMA as an accelerating agent to overcome the delay in the expansion that occurs in the presence of welan gum. Cheung et al. [92] noted that an accelerator should assist: (1) $Ca(OH)_2$ nucleation, having control over the saturation levels and influence the etch pit activation; (2) CSH nucleation, giving more growth sites and CSH growth after nucleation, giving permeable reaction products promoting faster reaction after the induction period.

As for the hydration of calcium chloride, products may be either CaO or $Ca(OH)_2$ depending on the water content.

$$CaCl_{2\,(s)} + H_2O_{(l)} \rightarrow CaO_{(s)} + 2HCl_{(aq)} \quad (22)$$

$$CaCl_{2\,(s)} + 2H_2O_{(l)} \rightarrow Ca(OH)_{2\,(s)} + HCl_{(aq)} \quad (23)$$

However, according to Kondo et al., these hydration reactions occur at a temperature of above 840 °C for the fused $CaCl_2$ [93]. Therefore, it can be concluded that $CaCl_2$ does not undergo hydration in the process and simply acts as an accelerator without interfering with the primary reaction of concern.

Regarding the acceleration behavior of $CaCl_2$, many articles have suggested that it can promote the dissolution of cement, accelerate the formation of hydration products, and increase the heat flow rate of tricalcium silicate hydration [94], shortening the pre-induction and induction period, leading to a faster expansion [13]. This suggests that $CaCl_2$ would promote the dissolution of specifically tricalcium silicate and accelerate the supersaturation of hydration products, triggering the initiation of acceleration of the hydration products by nucleation [95]. However, it contradicts the theoretical approach taken by considering the dissolution of $CaCl_2$ in water when the experimental observations are taken into consideration.

$$CaCl_{2\,(aq)} \rightarrow {Ca^{2+}}_{(aq)} + 2{Cl^{-}}_{(aq)} \quad (24)$$

Now considering the stoichiometric dissolution of tricalcium silicate,

$$3CaO{\cdot}SiO_{2\,(aq)} \rightleftharpoons 3{Ca^{2+}}_{(aq)} + {SiO_4}^{4-}{}_{(aq)} + {O^{2-}}_{(aq)} \quad (25)$$

Calcium chloride, being an inorganic ionic solid, dissolves in water completely and rapidly in comparison to tricalcium silicate. As tricalcium silicate dissolves in water, the water would already have a considerable concentration of Ca^{2+}, leading to a less effective dissolution, which can be explained by the common ion effect of the Le' Chatelier's principle. However, the effectiveness of $CaCl_2$ as an accelerator in the cement industry is well known [40,96]. Thus, a more complex mechanism of acceleration is expected. For example, the acceleration of expansion with the amount of $CaCl_2$ has been studied by de Silva et al. [13], and it has been observed that the expansive pressure development does not increase with the amount of $CaCl_2$ added but would reduce after an optimum quantity, again suggesting the complex mechanism. The studies conducted by Ramachandran et al. [97] regarding the morphological changes of the hydration products with increasing amounts of $CaCl_2$, might be useful in explaining the observations made by de Silva et al. [13]. It has been found that the morphology of the hydration products changes

from a needle shape to sheets, then plates and finally a sponge-like consistency at 0%, 1%, 2% and 5% $CaCl_2$, respectively, as shown in Figure 9. This weak porous structure observed in samples containing over 2% $CaCl_2$ clarifies the unexpected weak expansive pressure observed by de Silva et al. [13].

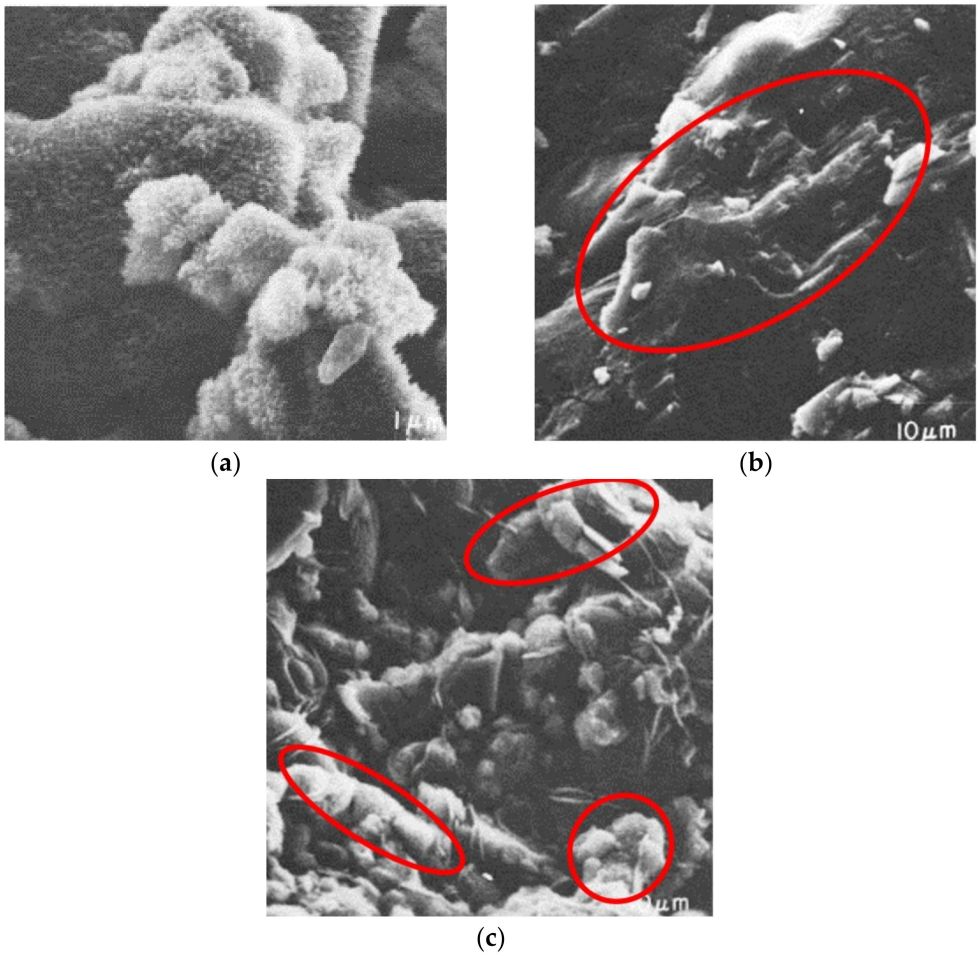

Figure 9. SEM images of the hydration products of alite in the presence of (**a**) 0% $CaCl_2$ giving small needles, (**b**) 2% $CaCl_2$ giving thick plates and (**c**) 5% $CaCl_2$ giving a spongey consistency [98].

Yet, reflecting upon at the mechanism of action of $CaCl_2$, according to the classical nucleation theory, heterogeneous nucleation takes place on the surface, depending on the contact angle between the precipitating phase and the surface [99]. However, the slow dissolution hypothesis proposes that there would be a greater degree of supersaturation of CSH prior to the supersaturation of $Ca(OH)_2$, and the precipitation occurs on the surfaces where CSH is supersaturated with respect to the solution.

Due to the high solubility of $CaCl_2$ in water and the ability of Ca^{2+} to interact in the crystallization process, the degree of supersaturation of CSH would increase in the presence of $CaCl_2$, leading to the activation of inactive sites and accelerating the steady state of Stage 2 [100]. Even after the precipitation of CSH and $Ca(OH)_2$, Ca^{2+} from $CaCl_2$ would remain in the solution as it is a catalyst. Therefore, the saturation levels of Ca^{2+} would be maintained allowing further precipitation of CSH, thus achieving all the requirements of an accelerator, provided by Cheung et al. [92].

5.4. Additives for Further Development of SREMA

As discussed in Section 3, SREMA has the capability to be further developed with other similar additives to meet certain energy and environmental conditions. Several of such additives and a brief understanding on how they would behave within SREMA, are analyzed in Table 3.

Table 3. Additives that can be considered for further development of SREMA.

Additive	Types Commonly Used in Cement Industry	Mechanism of Action
VEA	Silica-based slurry	Nano/micro silica particles would easily interact with the liquid phase of the cement mixture, forming a gel-like consistency, thereby increasing the retention of water [101]. As the particles fill the voids between cement particles, it would provide additional nucleation sites for hydration and create CSH phases [102]. Thus, the resulting volume expansion may be comparatively larger. However, the workability is greatly decreased with the addition of silica-based slurries [101].
	Ethylenoxide derivate	These organic VEAs would retain water and decrease the mass loss, similar to welan gum as discussed in the Section 5.1, due to the multiple O atoms in the structures [103]. However, the amylopectin branch of starch facilitates relatively low viscosity. Therefore, the amount of starch-derivative necessary would be about 10 times that of a polysaccharide [104].
	Other natural polysaccharides (diutan gum, xanthan gum)	
	Starch-based derivatives	
HRWR	Polycarboxylate-type	Polycarboxylate-derivatives would behave similar to SNSF in the presence of cement, with the carbonate group interacting with water. However, these derivatives would slow down the ettringite precipitation [105]. Since the carbonate group is stronger compared to sulfonate group (in SNSF), the adsorption of the anionic head into the active sites can be seen more frequently in the presence polycarboxylate-derivatives [106].
	Diphosphonate-type	The phosphonate groups would interact with water similar to SNSF. However, a slight increase in Ca^{2+} concentration in the system can be observed, in the presence of diphosphonate-derivatives. This is due to the complex formation between the diphosphonates and Ca^{2+} ions leading to further dissolution of the Ca-based compounds in cement [105].
Accelerator		Other cations of a similar size and charge, that are is a similar charge density, would also show an accelerated reaction mechanism [107]. Thus, the effectiveness of cations as a chemical accelerator is as follows [108,109]: $Ca^{2+} > Sr^{2+} > Ba^{2+} > Li^{+} > K^{+} > Na^{+} \approx Cs^{+} > Rb^{+}$ The counter ion which would maintain the electroneutrality of the sample, should not bind to either CSH or alite during the hydration process, by replacing the silicates. As silicates are covalently bonded, highly electronegative anions such as bromides and chlorides would not take their position while anions that are less electronegative such as fluorides would replace silicates, inhibiting the acceleration [110]. Therefore, the effectiveness of anions as a chemical accelerator is as follows: $Br^{-} \approx Cl^{-} > SCN^{-} > I^{-} > NO_3{}^{-} > ClO_4{}^{-}$ However, considering $CaBr_2$ and $CaCl_2$, the chloride dissolves more efficiently and therefore is used in cement industry.

6. Conclusions

This review has attempted to study the mechanisms of action of the non-destructive and self-expansive product, SREMA. Through numerous studies conducted on expansive materials, it is evident that the expansive nature of SREMA results from the hydration of CaO- and CaO-based minerals. According to the conducted review, the main conclusions can be summarized as follows.

The main volume expansive components of SREMA are calcium hydroxide and ettringite, which are formed by the hydration of calcium oxide, alite and tricalcium aluminate.

The hydration mechanisms of calcium oxide and tricalcium aluminate are straightforward, while the ambiguities in the hydration alite are addressed by the slow dissolution hypothesis.

The combined hydration mechanism of alite and tricalcium aluminate show sensitivity towards compositional as well as environmental changes.

Welan gum successfully retains water and reduces the mass loss of SREMA. It is also capable of increasing the viscosity when mixed with a HRWR, such as SNSF. However, the retardation of the hydration reaction due to polymer adsorption can be overcome with a suitable accelerator.

Calcium chloride, used as the accelerator, improves the Ca^{2+} ion concentration in the solution enabling CSH supersaturation and thereby accelerating the product formation.

Moving towards a sustainable future, SREMA has gained attention and popularity by minimizing the irreversible mutilations to the Earth's ecosystem that can be seen with the use of conventional mining techniques. With the multiple uses of SREMA on the same borehole, the rock fracturing process can be extended to a larger underground area without inducing seismic activities. Thus, with further studies, SREMA has the potential to adapt according to the necessary ground conditions.

Author Contributions: The initial draft of the review paper was done by J.B.L. The drafted manuscript was reviewed and corrected by R.P.G. The concept was conceived by R.P.G. who also carried out the final check of the review paper. All authors have read and agreed to the published version of the manuscript.

Funding: This research received no external funding.

Conflicts of Interest: The authors declare no conflict of interest. The founding sponsors had no role in the design of the study; in the collection, analyses, or interpretation of data; in the writing of the manuscript, and in the decision to publish the results.

References

1. Holland, A.A. Earthquakes Triggered by Hydraulic Fracturing in South-Central Oklahoma. *Bull. Seismol. Soc. Am.* **2013**, *103*, 1784–1792. [CrossRef]
2. Inoue, H.; Lisitsyn, I.V.; Akiyama, H.; Nishizawa, I. Pulsed Electric Breakdown and Destruction of Granite. *Jpn. J. Appl. Phys.* **1999**, *38*, 6502. [CrossRef]
3. Winter, T.; Harvey, J.; Franke, O.; Alley, W. *Ground Water and Surface Water: A Single Resource, Circular 1139*; DIANE Publishing Inc.: Collingdale, PA, USA, 1998.
4. Cooley, H.; Donnelly, K.; Ross, N.; Luu, P. *Hydraulic Fracturing and Water Resources: Separating the Frack from the Fiction*; Pacific Institute: Oakland, CA, USA, 2012.
5. Levy, S.M. Calculations Relating to Concrete and Masonry. In *Construction Calculations Manual*; Butterworth-Heinemann: Oxford, UK, 2012; pp. 211–264.
6. Bentur, A.; Ish-Shalom, M. Properties of Type K Expensive Cement of Pure Components II-Proposed Mechanism of Ettringite Formation and Expansion in Unrestrained Paste of Pure Expansive Component. *Cem. Concr. Res.* **1974**, *4*, 709–721. [CrossRef]
7. Cohen, M. Modeling of Expansive Cements. *Cem. Concr. Res.* **1983**, *13*, 519–528. [CrossRef]
8. Tang, S.; Huang, R.; Wang, S.; Bao, C.; Tang, C. Study of the Fracture Process in Heterogeneous Materials Around Boreholes Filled with Expansion Cement. *Int. J. Solids Struct.* **2017**, *112*, 1–15. [CrossRef]
9. Hinze, J.; Brown, J. Properties of Soundless Chemical Demolition Agents. *J. Constr. Eng. Manag.* **1994**, *120*, 816–827. [CrossRef]
10. Gambatese, J.A. Controlled Concrete Demolition Using Expansive Cracking Agents. *J. Constr. Eng. Manag.* **2003**, *129*, 98–104. [CrossRef]
11. De Silva, V.; Ranjith, P.; Perera, M.; Wu, B.; Rathnaweera, T. Investigation of the Mechanical, Microstructural and Mineralogical Morphology of Soundless Cracking Demolition Agents during the Hydration Process. *Mater. Charact.* **2017**, *130*, 9–24. [CrossRef]
12. Laefer, D.F.; Ambrozevitch-Cooper, N.; Huynh, M.; Midgette, J.; Ceribasi, S.; Wortman, J. Expansive Fracture Agent Behaviour for Concrete Cracking. *Mag. Concr. Res.* **2010**, *62*, 443–452. [CrossRef]
13. De Silva, V.; Ranjith, P.; Perera, M.; Wu, B.; Rathnaweera, T. A Modified, Hydrophobic Soundless Cracking Demolition Agent for Non-explosive Demolition and Fracturing Applications. *Process. Saf. Environ. Prot.* **2018**, *119*, 1–13. [CrossRef]
14. Gamage, R.P.; De Silva, R.S.V. Demolition Agent. U.S. Patent 10836955B2, 17 November 2020.
15. Sinclair, L.; Thompson, J. In Situ Leaching of Copper: Challenges and Future Prospects. *Hydrometallurgy* **2015**, *157*, 306–324. [CrossRef]

16. Zhou, Y.; Li, G.; Xu, L.; Liu, J.; Sun, Z.; Shi, W. Uranium Recovery from Sandstone-Type Uranium Deposit by Acid In-Situ Leaching-An Example from the Kujieertai. *Hydrometallurgy* **2020**, *191*, 105209. [CrossRef]
17. De Rouffignac, E.P.; Vinegar, H.J.; Wellington, S.L.; Karanikas, J.M.; Berchenko, I.E.; Maher, K.A.; Zhang, E.; Fowler, T.D.; Keedy, C.R.; Ryan, R.C.; et al. In Situ Thermal Processing of a Coal Formation Using Heat Sources Positioned within Open Wellbores. U.S. Patent 6,752,210, 22 June 2004.
18. Hall, A.; Scott, J.A.; Shang, H. Geothermal Energy Recovery from Underground Mines. *Renew. Sustain. Energy Rev.* **2011**, *15*, 916–924. [CrossRef]
19. Sun, F.; Yao, Y.; Li, G.; Li, X. Performance of Geothermal Energy Extraction in a Horizontal Well by Using CO_2 as the Working Fluid. *Energy Convers. Manag.* **2018**, *171*, 1529–1539. [CrossRef]
20. Wang, K.; Yuan, B.; Ji, G.; Wu, X. A Comprehensive Review of Geothermal Energy Extraction and Utilization in Oilfields. *J. Pet. Sci. Eng.* **2018**, *168*, 465–477. [CrossRef]
21. Harada, T.; Soeda, K.; Idemitsu, T.; Watanabe, A. Characteristics of Expansive Pressure of an Expansive Demolition Agent and the Development of New Pressure Transducers. *Doboku Gakkai Ronbunshu* **1993**, *1993*, 91–100. [CrossRef]
22. Natanzi, A.S.; Laefer, D.F.; Connolly, L. Cold and Moderate Ambient Temperatures Effects on Expansive Pressure Development in Soundless Chemical Demolition Agents. *Constr. Build. Mater.* **2016**, *110*, 117–127. [CrossRef]
23. Collepardi, M.; Borsoi, A.; Collepardi, S.; Olagot, J.J.O.; Troli, R. Effects of Shrinkage Reducing Admixture in Shrinkage Compensating Concrete under Non-Wet Curing Conditions. *Cem. Concr. Compos.* **2005**, *27*, 704–708. [CrossRef]
24. Chatterji, S. Mechanism of Expansion of Concrete Due to the Presence of Dead-Burnt CaO and MgO. *Cem. Concr. Res.* **1995**, *25*, 51–56. [CrossRef]
25. El Dessouki, A.; Mitri, H. Rock Breakage Using Expansive Cement. *Engineering* **2011**, *3*, 168–173. [CrossRef]
26. Hirota, T.; Ishizaki, Y. Static Expansive Demolition Agent in the Three-Dimensional Form and Process for Demolishing Brittle Material Using the Same. U.S. Patent 4,600,154, 15 July 1986.
27. Ishii, S.; Kubota, H.; Hida, T.; Migita, J. Expansive Demolition Agent. U.S. Patent 4807530A, 28 February 1989.
28. Chang, S.-H.; Lee, C.-I.; Jeon, S. Measurement of Rock Fracture Toughness under Modes I and II and Mixed-Mode Conditions by Using Disc-Type Specimens. *Eng. Geol.* **2002**, *66*, 79–97. [CrossRef]
29. Xu, Y.; Chung, D. Effect of Sand Addition on the Specific Heat and Thermal Conductivity of Cement. *Cem. Concr. Res.* **2000**, *30*, 59–61. [CrossRef]
30. Arefi, M.; Javeri, M.; Mollaahmadi, E. To Study the Effect of Adding Al2O3 Nanoparticles on the Mechanical Properties and Microstructure of Cement Mortar. *Life Sci. J.* **2011**, *8*, 613–617.
31. De Silva, V.; Ranjith, P.; Perera, M.; Wu, B.; Rathnaweera, T. The Influence of Admixtures on the Hydration Process of Soundless Cracking Demolition Agents (SCDA) for Fragmentation of Saturated Deep Geological Reservoir Rock Formations. *Rock Mech. Rock Eng.* **2019**, *52*, 435–454. [CrossRef]
32. Campana, S.; Andrade, C.; Milas, M.; Rinaudo, M. Polyelectrolyte and Rheological Studies on the Polysaccharide Welan. *Int. J. Biol. Macromol.* **1990**, *12*, 379–384. [CrossRef]
33. Sandford, P.A.; Cottrell, I.W.; Pettitt, D.J. Microbial Polysaccharides: New Products and Their Commercial Applications. *Pure Appl. Chem.* **1984**, *56*, 879–892. [CrossRef]
34. Khayat, K.H.; Yahia, A. Simple Field Tests to Characterize Fluidity and Washout Resistance of Structural Cement Grout. *Cem. Concr. Aggreg.* **1998**, *20*, 145–156.
35. Sakata, N.; Yanai, S.; Yokozeki, K.; Maruyama, K. Study on New Viscosity Agent for Combination Use Type of Self-Compacting Concrete. *J. Adv. Concr. Technol.* **2003**, *1*, 37–41. [CrossRef]
36. Rakitsky, W.G.; Richey, D.D. Rapidly Hydrating Welan Gum. CA2063087C, 21 May 2002.
37. Kaur, V.; Bera, M.B.; Panesar, P.S.; Kumar, H.; Kennedy, J. Welan Gum: Microbial Production, Characterization, and Applications. *Int. J. Biol. Macromol.* **2014**, *65*, 454–461. [CrossRef] [PubMed]
38. Ma, L.; Zhao, Q.; Yao, C.; Zhou, M. Impact of Welan Gum on Tricalcium Aluminate-Gypsum Hydration. *Mater. Charact.* **2012**, *64*, 88–95. [CrossRef]
39. Giergiczny, Z. Effect of Some Additives on the Reactions in Fly Ash-Ca (OH) 2 System. *J. Therm. Anal. Calorim.* **2004**, *76*, 747–754. [CrossRef]
40. Peterson, V.K.; Juenger, M.C.G. Hydration of Tricalcium Silicate: Effects of $CaCl_2$ and Sucrose on Reaction Kinetics and Product Formation. *Chem. Mater.* **2006**, *18*, 5798–5804. [CrossRef]
41. Arshadnejad, S.; Goshtasbi, K.; Aghazadeh, J. A Model to Determine Hole Spacing in the Rock Fracture Process by Non-explosive Expansion Material. *Int. J. Miner. Metall. Mater.* **2011**, *18*, 509–514. [CrossRef]
42. Cuesta, A.; Zea-Garcia, J.D.; Londono-Zuluaga, D.; Angeles, G.; Santacruz, I.; Vallcorba, O.; Dapiaggi, M.; Sanfélix, S.G.; Aranda, M.A. Multiscale Understanding of Tricalcium Silicate Hydration Reactions. *Sci. Rep.* **2018**, *8*, 1–11.
43. Bazzoni, A.; Cantoni, M.; Scrivener, K.L. Impact of Annealing on the Early Hydration of Tricalcium Silicate. *J. Am. Ceram. Soc.* **2014**, *97*, 584–591. [CrossRef]
44. Pustovgar, E.; Mishra, R.K.; Palacios, M.; de Lacaillerie, J.-B.d.E.; Matschei, T.; Andreev, A.S.; Heinz, H.; Verel, R.; Flatt, R.J. Influence of Aluminates on the Hydration Kinetics of Tricalcium Silicate. *Cem. Concr. Res.* **2017**, *100*, 245–262. [CrossRef]
45. Taylor, H.F. *Cement chemistry*; Thomas Telford Ltd.: London, UK, 1997; Volume 2.

46. Ángeles, G.; De Vera, R.N.; Cuberos, A.J.; Aranda, M.A. Crystal Structure of Low Magnesium-Content Alite: Application to Rietveld Quantitative Phase Analysis. *Cem. Concr. Res.* **2008**, *38*, 1261–1269.
47. Bullard, J.W.; Jennings, H.M.; Livingston, R.A.; Nonat, A.; Scherer, G.W.; Schweitzer, J.S.; Scrivener, K.L.; Thomas, J.J. Mechanisms of Cement Hydration. *Cem. Concr. Res.* **2011**, *41*, 1208–1223. [CrossRef]
48. Jennings, H.M. Aqueous Solubility Relationships for Two Types of Calcium Silicate Hydrate. *J. Am. Ceram. Soc.* **1986**, *69*, 614–618. [CrossRef]
49. Bullard, J.W. A Determination of Hydration Mechanisms for Tricalcium Silicate Using a Kinetic Cellular Automaton Model. *J. Am. Ceram. Soc.* **2008**, *91*, 2088–2097. [CrossRef]
50. Kantro, D.L.; Brunauer, S.; Weise, C.H. Development of Surface in the Hydration of Calcium Silicates. II. Extension of Investigations to Earlier and Later Stages of Hydration. *J. Phys. Chem.* **1962**, *66*, 1804–1809. [CrossRef]
51. Stein, H.; Stevels, J. Influence of Silica on the Hydration of 3 CaO, SiO_2. *J. Appl. Chem.* **1964**, *14*, 338–346. [CrossRef]
52. Gartner, E.M.; Jennings, H.M. Thermodynamics of Calcium Silicate Hydrates and Their Solutions. *J. Am. Ceram. Soc.* **1987**, *70*, 743–749. [CrossRef]
53. Birchall, J.D.; Howard, A.; Bailey, J. On the Hydration of Portland Cement. *Proc. R. Soc. London A. Math. Phys. Sci.* **1978**, *360*, 445–453.
54. Garrault, S.; Finot, E.; Lesniewska, E.; Nonat, A. Study of CSH Growth on C 3 S Surface during Its Early Hydration. *Mater. Struct.* **2005**, *38*, 435–442. [CrossRef]
55. Lesko, S.; Lesniewska, E.; Nonat, A.; Mutin, J.-C.; Goudonnet, J.-P. Investigation by Atomic Force Microscopy of Forces at the Origin of Cement Cohesion. *Ultramicroscopy* **2001**, *86*, 11–21. [CrossRef]
56. Juilland, P.; Gallucci, E.; Flatt, R.; Scrivener, K. Dissolution Theory Applied to the Induction Period in Alite Hydration. *Cem. Concr. Res.* **2010**, *40*, 831–844. [CrossRef]
57. Marchon, D.; Flatt, R.J. Mechanisms of Cement Hydration. In *Science and Technology of Concrete Admixtures*; Elsevier: Amsterdam, The Netherlands, 2016; pp. 129–145.
58. Tadros, M.; Skalny, J.; Kalyoncu, R. Early Hydration of Tricalcium Silicate. *J. Am. Ceram. Soc.* **1976**, *59*, 344–347. [CrossRef]
59. Zheng, L.; Xuehua, C.; Mingshu, T. Hydration and Setting Time of MgO-Type Expansive Cement. *Cem. Concr. Res.* **1992**, *22*, 1–5. [CrossRef]
60. Mo, L.; Deng, M.; Tang, M.; Al-Tabbaa, A. MgO Expansive Cement and Concrete in China: Past, Present and Future. *Cem. Concr. Res.* **2014**, *57*, 1–12. [CrossRef]
61. Bullard, J.W.; Flatt, R.J. New Insights into the Effect of Calcium Hydroxide Precipitation on the Kinetics of Tricalcium Silicate Hydration. *J. Am. Ceram. Soc.* **2010**, *93*, 1894–1903. [CrossRef]
62. Garrault, S.; Nonat, A. Hydrated Layer Formation on Tricalcium and Dicalcium Silicate Surfaces: Experimental Study and Numerical Simulations. *Langmuir* **2001**, *17*, 8131–8138. [CrossRef]
63. Thomas, J.J.; Jennings, H.M.; Chen, J.J. Influence of Nucleation Seeding on the Hydration Mechanisms of Tricalcium Silicate and Cement. *J. Phys. Chem. C* **2009**, *113*, 4327–4334. [CrossRef]
64. Garrault, S.; Behr, T.; Nonat, A. Formation of the C− S− H Layer during Early Hydration of Tricalcium Silicate Grains with Different Sizes. *J. Phys. Chem. B* **2006**, *110*, 270–275. [CrossRef]
65. Meredith, P.; Donald, A.; Meller, N.; Hall, C. Tricalcium Aluminate Hydration: Microstructural Observations by In-Situ Electron Microscopy. *J. Mater. Sci.* **2004**, *39*, 997–1005. [CrossRef]
66. Maier, A.-K.; Dezmirean, L.; Will, J.; Greil, P. Three-Dimensional Printing of Flash-Setting Calcium Aluminate Cement. *J. Mater. Sci.* **2011**, *46*, 2947–2954. [CrossRef]
67. Bickmore, B.R.; Nagy, K.L.; Gray, A.K.; Brinkerhoff, A.R. The Effect of Al (OH) 4−on the Dissolution Rate of Quartz. *Geochim. Et Cosmochim. Acta* **2006**, *70*, 290–305. [CrossRef]
68. Begarin, F.; Garrault, S.; Nonat, A.; Nicoleau, L. Hydration of Alite Containing Aluminium. *Adv. Appl. Ceram.* **2011**, *110*, 127–130. [CrossRef]
69. Matschei, T.; Lothenbach, B.; Glasser, F. The AFm Phase in Portland Cement. *Cem. Concr. Res.* **2007**, *37*, 118–130. [CrossRef]
70. Pourchet, S.; Regnaud, L.; Perez, J.-P.; Nonat, A. Early C3A Hydration in the Presence of Different Kinds of Calcium Sulfate. *Cem. Concr. Res.* **2009**, *39*, 989–996. [CrossRef]
71. Skalny, J.; Tadros, M. Retardation of Tricalcium Aluminate Hydration by Sulfates. *J. Am. Ceram. Soc.* **1977**, *60*, 174–175. [CrossRef]
72. Mehta, P. Morphology of Calcium Sulfoaluminate Hydrates. *J. Am. Ceram. Soc.* **1969**, *52*, 521–522. [CrossRef]
73. Collepardi, M.; Baldini, G.; Pauri, M.; Corradi, M. Tricalcium Aluminate Hydration in the Presence of Lime, Gypsum or Sodium Sulfate. *Cem. Concr. Res.* **1978**, *8*, 571–580. [CrossRef]
74. Scrivener, K.L.; Nonat, A. Hydration of Cementitious Materials, Present and Future. *Cem. Concr. Res.* **2011**, *41*, 651–665. [CrossRef]
75. Manzano, H.; Dolado, J.S.; Ayuela, A. Structural, Mechanical, and Reactivity Properties of Tricalcium Aluminate Using First-Principles Calculations. *J. Am. Ceram. Soc.* **2009**, *92*, 897–902. [CrossRef]
76. Minard, H.; Garrault, S.; Regnaud, L.; Nonat, A. Mechanisms and Parameters Controlling the Tricalcium Aluminate Reactivity in the Presence of Gypsum. *Cem. Concr. Res.* **2007**, *37*, 1418–1426. [CrossRef]
77. Lerch, W. The Influence of Gypsum on the Hydration and Properties of Portland Cement Pastes. *Proc. Am. Soc. Test. Mater.* **2008**, *46*, 1252–1291.

78. Quennoz, A.; Scrivener, K.L. Interactions between Alite and C3A-Gypsum Hydrations in Model Cements. *Cem. Concr. Res.* **2013**, *44*, 46–54. [CrossRef]
79. Scrivener, K.L.; Pratt, P. Microstructural Studies of the Hydration of C 3 A and C 4 AF Independently and in Cement Paste. *Proc. Proc. Br. Ceram. Soc.* **1984**, *35*, 207.
80. Jansson, P.-E.; Lindberg, B.; Widmalm, G.; Sandford, P.A. Structural Studies of an Extracellular Polysaccharide (S-130) Elaborated by Alcaligenes ATCC 31555. *Carbohydr. Res.* **1985**, *139*, 217–223. [CrossRef]
81. Zhang, Y.; Liu, C.; Luping, Z.; Qu, C.; Zhao, Q. The impact of welan gum on C3S hydration system. In Proceedings of the 15th International Congress on the Chemistry of Cement, Budapest, Hungary, 15 July 2017; p. 353.
82. Kurozumi, M.; Sugimori, D. Biodegradation of Anionic Surfactant, Sodium 2-Naphthalene Sulfonate Formaldehyde Condensates, by the Fungus Cunning-Hamella Polymorpha. *Sen'i Gakkaishi* **2000**, *56*, 109–111. [CrossRef]
83. Peng, X.; Li, X.; Chen, D.; Ma, D. Effect of Side Chains on the Dispersing Properties of Polycarboxylate-Type Superplasticisers in Cement Systems. *Mag. Concr. Res.* **2013**, *65*, 422–429. [CrossRef]
84. Winnefeld, F.; Becker, S.; Pakusch, J.; Götz, T. Effects of the Molecular Architecture of Comb-Shaped Superplasticizers on Their Performance in Cementitious Systems. *Cem. Concr. Compos.* **2007**, *29*, 251–262. [CrossRef]
85. Tan, H.; Huang, J.; Ma, B.; Li, X. Effect of Superplasticiser and Sodium Tripolyphosphate on Fluidity of Cement Paste. *Mag. Concr. Res.* **2014**, *66*, 1194–1200. [CrossRef]
86. Yamada, K.; Ogawa, S.; Hanehara, S. Controlling of the Adsorption and Dispersing Force of Polycarboxylate-Type Superplasticizer by Sulfate Ion Concentration in Aqueous Phase. *Cem. Concr. Res.* **2001**, *31*, 375–383. [CrossRef]
87. Vovk, A.; Ushenov-Marshak, A. Physicochemical Characteristics of Hydration of Low-Water-Demand Binders. *Neorg. Mater.* **1993**, *29*, 708–716.
88. Sakai, E.; Raina, K.; Asaga, K.; Goto, S.; Kondo, R. Influence of Sodium Aromatic Sulfonates on the Hydration of Tricalcium Aluminate with or without Gypsym. *Cem. Concr. Res.* **1980**, *10*, 311–319. [CrossRef]
89. Hekal, E.E.; Kishar, E.A. Effect of Sodium Salt of Naphthalene-Formaldehyde Polycondensate on Ettringite Formation. *Cem. Concr. Res.* **1999**, *29*, 1535–1540. [CrossRef]
90. Collepardi, M.; Monosi, S.; Moriconi, G.; Corradi, M. Combined Effect of Lignosulfonate and Carbonate on Pure Portland Clinker Compounds Hydration. I-Tetracalcium Aluminoferrite Hydration. *Cem. Concr. Res.* **1980**, *10*, 455–462. [CrossRef]
91. Plank, J.; Lummer, N.R.; Dugonjić-Bilić, F. Competitive Adsorption Between an AMPS®-Based Fluid Loss Polymer and Welan Gum Biopolymer in Oil Well Cement. *J. Appl. Polym. Sci.* **2010**, *116*, 2913–2919. [CrossRef]
92. Cheung, J.; Jeknavorian, A.; Roberts, L.; Silva, D. Impact of Admixtures on the Hydration Kinetics of Portland Cement. *Cem. Concr. Res.* **2011**, *41*, 1289–1309. [CrossRef]
93. Kondo, H.; Asaki, Z.; Kondo, Y. Hydrolysis of Fused Calcium Chloride at High Temperature. *Metall. Trans. B* **1978**, *9*, 477–483. [CrossRef]
94. Robin, V.; Wild, B.; Daval, D.; Pollet-Villard, M.; Nonat, A.; Nicoleau, L. Experimental Study and Numerical Simulation of the Dissolution Anisotropy of Tricalcium Silicate. *Chem. Geol.* **2018**, *497*, 64–73. [CrossRef]
95. Juenger, M.; Monteiro, P.; Gartner, E.; Denbeaux, G. A Soft X-ray Microscope Investigation into the Effects of Calcium Chloride on Tricalcium Silicate Hydration. *Cem. Concr. Res.* **2005**, *35*, 19–25. [CrossRef]
96. Onuaguluchi, O.; Ratu, R.; Banthia, N. The Effects of CaCl 2-Blended Acrylic Polymer Emulsion on the Properties of Cement Mortar. *Mater. Struct.* **2018**, *51*, 1–10. [CrossRef]
97. Ramachandran, V.S.; Feldman, R.F. *Time-Dependent and Intrinsic Characteristics of Portland Cement Hydrated in the Presence of Calcium Chloride*; National Research Council: Ottawa, ON, Canada, 1978.
98. Traetteberg, A.; Ramachandran, V.S.; Grattan-Bellew, P. A Study of the Microstructure and Hydration Characteristics of Tricalcium Silicate in the Presence of Calcium Chloride. *Cem. Concr. Res.* **1974**, *4*, 203–221. [CrossRef]
99. Markov, I. Crystal Growth for Beginners: Fundamentals of Nucleation. In *Growth and Epitaxy*; World Scientific: Singapore, 2003.
100. Vehmas, T.; Kronlöf, A. A Study of Early-Age Ordinary Portland Cement Hydration According to Autocatalytic Reaction Model. *Nord. Concr. Res.* **2011**, *43*, 269–272.
101. Berra, M.; Carassiti, F.; Mangialardi, T.; Paolini, A.; Sebastiani, M. Effects of Nanosilica Addition on Workability and Compressive Strength of Portland Cement Pastes. *Constr. Build. Mater.* **2012**, *35*, 666–675. [CrossRef]
102. Bayanak, M.; Zarinabadi, S.; Shahbazi, K.; Azimi, A. Effects of Nano Silica on Oil Well Cement Slurry Charactreistics and Control of Gas Channeling. *South. Afr. J. Chem. Eng.* **2020**, *34*, 11–25. [CrossRef]
103. Khayat, K.H. Viscosity-Enhancing Admixtures for Cement-Based Materials-An Overview. *Cem. Concr. Compos.* **1998**, *20*, 171–188. [CrossRef]
104. Isik, I.E.; Ozkul, M.H. Utilization of Polysaccharides as Viscosity Modifying Agent in Self-Compacting Concrete. *Constr. Build. Mater.* **2014**, *72*, 239–247. [CrossRef]
105. Pourchet, S.; Comparet, C.; Nicoleau, L.; Nonat, A. Influence of PC superplasticizers on tricalcium silicate hydration. In Proceedings of the 12th International Congress on the Chemistry of Cement (ICCC 2007), Montreal, QC, Canada, 8–13 July 2007.
106. Simard, M.-A.; Nkinamubanzi, P.-C.; Jolicoeur, C.; Perraton, D.; Aïtcin, P.-C. Calorimetry, Rheology and Compressive Strength of Superplasticized Cement Pastes. *Cem. Concr. Res.* **1993**, *23*, 939–950. [CrossRef]
107. Vehmas, T.; Kronlöf, A.; Cwirzen, A. Calcium Chloride Acceleration in Ordinary Portland Cement. *Mag. Concr. Res.* **2018**, *70*, 856–863. [CrossRef]

108. Wilding, C.; Walter, A.; Double, D. A Classification of Inorganic and Organic Admixtures by Conduction Calorimetry. *Cem. Concr. Res.* **1984**, *14*, 185–194. [CrossRef]
109. Double, D. New Developments in Understanding the Chemistry of Cement Hydration. *Philos. Trans. R. Soc. London. Ser. A Math. Phys. Sci.* **1983**, *310*, 53–66.
110. Fujioka, I.; Imada, K.; Nishimura, M.; Ishibashi, T. Nonexplosive Chemical Composition for Gently Breaking Rock or Concrete Mass. U.S. Patent 4,565,579, 21 January 1986.